Precise Fault Location on Transmission Lines Using Ensemble Kalman Filter

Rui Fan, *Member, IEEE*, Yu Liu, *Member, IEEE*, Renke Huang, *Member, IEEE*, Ruisheng Diao, *Senior Member, IEEE*, and Shaobu Wang, *Member, IEEE*

***Abstract*—Accurate pin-pointing of faults on transmission lines minimizes outage time, labor, and costs. This letter proposes a simple yet effective ensemble Kalman filter (EnKF) approach to accurately locating the faults on transmission lines within half-cycle time. The approach is easy to implement and does not require foreknowledge of either the fault type or an approximate guess of the fault location. Extensive results validate the effectiveness and accuracy of the EnKF-based fault location approach.**

***Index Terms*—Dynamic state estimation, ensemble Kalman filter, fault location, fault classification.**

I. Introduction

TRANSMISSION line fault location techniques are mainly classified into three categories: single-ended impedance method, dual-ended impedance method [1], and traveling wave method [2]. Single-ended or dual-ended impedance methods use the fundamental frequency of phasor measurements at one or two terminals of lines to determine the fault location by calculating the impedance from the fault point to the terminal. The performance is affected by fault path resistance, loading, and source parameters. The traveling wave method monitors the wave arrival times to determine the fault location. However, this method requires super-high sampling rate, and the result accuracy is questionable when the fault occurs close to bus.

In [3] the fault distance is treated as a state of dynamic state estimation (DSE) process in which a weighted least square (WLS) method is used. However, the WLS-based method has several disadvantages: (1) it has to know the exact fault types and a close guess of the fault distance to initiate the state estimation, (2) the formulation of the Jacobian matrix is very complicated, and (3) WLS is typically better suited for static state estimation rather than DSE and may cause problems for nonlinear state estimations.

In this letter, we propose a two-step EnKF approach to avoid the above disadvantages. The first step determines the fault type and gets an initial estimation of the fault location. The second step involves performing a reinforced EnKF to determine an accurate fault location. This method does not require foreknowledge of either the fault type or an approximate guess of the fault location, and it only needs a data window of half cycle and is easy to be implemented without deriving the Jacobian matrix.

Manuscript received November 30, 2017; revised February 12, 2018 and April 26, 2018; accepted May 26, 2018. Date of publication June 22, 2018; date of current version November 20, 2018. This work was supported by PNNL Quickstarter Program. Paper no. PESL-00238-2017. *(Corresponding author: Rui Fan.)*

R. Fan, R. Huang, R. Diao, and S. Wang are with the Pacific Northwest National Laboratory, Richland, WA 99354 USA (e-mail: Rui.Fan@pnnl.gov; Renke.Huang@pnnl.gov; Ruisheng.diao@pnnl.gov; Shaobu.Wang@pnnl.gov).

Y. Liu is with the ShanghaiTech University, Shanghai 201210, China (e-mail: liuyu@shanghaitech.edu.cn).

Color versions of one or more of the figures in this letter are available online at http://ieeexplore.ieee.org.

Digital Object Identifier 10.1109/TPWRD.2018.2849879

II. Proposed Approach

The EnKF-based approach uses ensembles to represent and propagate the distribution of states [4]. Compared to the WLS, the EnKF eliminates the need to derive Jacobian matrices for nonlinear models and thereby the complexity of algorithm implementation. In addition, this approach leverages a full evolution of model non-linearity and error statistics, providing more accurate estimation and better numerical stability [5].

A. EnKF-Based Method

Given the transmission line model and measurements

$$x_k = f(x_{k-1}, u_{k-1}) + w_{k-1} \tag{1}$$

$$z_k = h(x_k, u_k) + v_{k-1} \tag{2}$$

where x is the states, u is the inputs, z is the measurements, k is the step number, w, v are the process and observation noises with zero mean and covariance of Q_d, R_d, f and h are the mapping or functions. Ensembles are formulated as an $n \times N$ matrix with the form of $X = [x_1, \ldots, x_N]$, where n is the state dimension and N is the number of samples. In this letter we selected a multi-section transmission line model for demonstration, without losing generality. Equations (1)–(2) are the discretization of the line model differential algebraic equations that are presented in [3].

When a fault occurs on a transmission line, the distance from the fault to the terminal is treated as a new state α that is invariant during the fault. The new model becomes

$$\begin{bmatrix} x_k \\ \alpha_k \end{bmatrix} = \begin{bmatrix} f(x_{k-1}, u_{k-1}, \alpha_{k-1}) + w_{k-1} \\ \alpha_{k-1} + w_{\alpha,k-1} \end{bmatrix}. \tag{3}$$

Note that the non-linearity of the model increases when α is introduced as a state. Defining an expanded vector of state as $y = (x, \alpha)^\top$. Equations (1) and (2) can be rewritten as

$$y_k = f(y_{k-1}, u_{k-1}) + w_{k-1} \tag{4}$$

$$z_k = h(y_k, u_k) + v_{k-1} \tag{5}$$

0885-8977 © 2018 IEEE. Personal use is permitted, but republication/redistribution requires IEEE permission.
See http://www.ieee.org/publications_standards/publications/rights/index.html for more information.

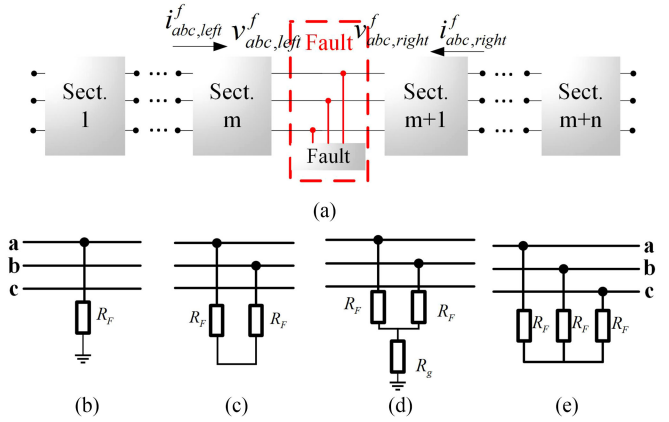

Fig. 1. (a) Multisection transmission line model. (b) Single-phase to ground. (c) Phase to phase. (d) Phase-to-phase to ground. (e) Three-phase faults.

The EnKF-based DSE can be summarized using an iterative prediction-correction process as follows:

EnKF Prediction:

$$y_k^{i-} = f\left(y_{k-1}^{i-}, u_{k-1}\right) + w_{k-1}^{i}, \tag{6}$$

$$z_k^{i-} = h\left(y_k^{i-}, u_k\right) + v_{k-1}^{i}, \tag{7}$$

$$\overline{y_k} = \frac{1}{N}\sum_{i=1}^{N} y_k^{i-}, \tag{8}$$

$$\overline{z_k} = \frac{1}{N}\sum_{i=1}^{N} z_k^{i-}; \tag{9}$$

EnKF Correction:

$$\overline{P_k}H_k^{\top} = \frac{1}{N}\sum_{i=1}^{N}\left(y_k^{i-} - \overline{y_k}\right)\left(z_k^{i-} - \overline{z_k}\right)^{\top}, \tag{10}$$

$$H_k\overline{P_k}H_k^{\top} = \frac{1}{N}\sum_{i=1}^{N}\left(z_k^{i-} - \overline{z_k}\right)\left(z_k^{i-} - \overline{z_k}\right)^{\top}, \tag{11}$$

$$K_k = \overline{P_k}H_k^{\top}\left(H_k\overline{P_k}H_k^{\top} + R_d\right)^{-1}, \tag{12}$$

$$y_k^{i} = y_k^{i-} + K_k\left(z_k^{i} - z_k^{i-}\right). \tag{13}$$

where P_k is the error covariance matrix, H_k is the Jacobian matrix, K_k is the Kalman gain, and the superscript notation $i-$ in y^{i-} or z^{i-} means that states and observations are computed in the prediction step. Note the Jacobian matrix H_k does not need to be derived explicitly from the non-linear equations.

B. Fault Classification and Reinforced Location

A simple two-step EnKF approach is proposed to avoid the disadvantages of the WLS-based method.

The first step determines the fault type and gets an initial estimation of the fault location. Transmission line faults can be classified into four categories: single-phase to ground, phase to phase, phase-to-phase to ground, and three-phase faults, as shown in Fig. 1. The multi-section transmission line models for

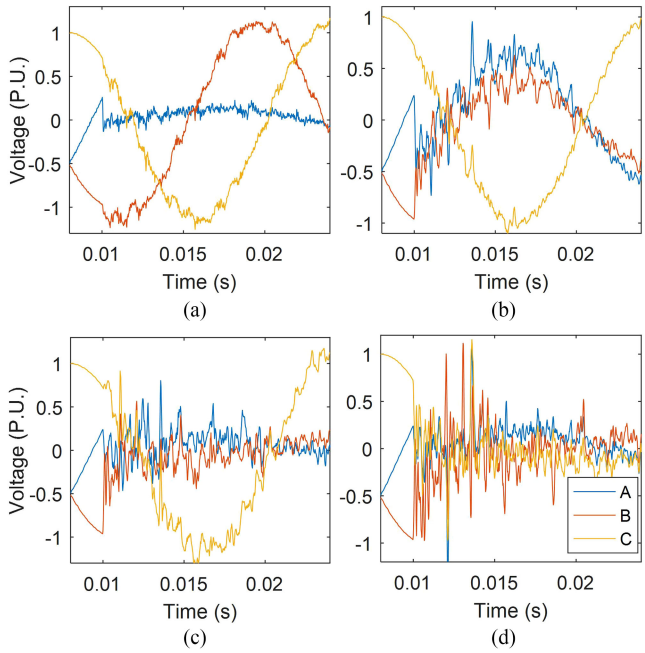

Fig. 2. Estimated fault point voltages for different fault types.

the pre-fault and post-fault conditions are slightly different at the faulted section connection point. The three-phase voltages and currents at health (un-faulted) section connection points always equal,

$$0 = v_{abc,left}^{sec,i}(t) - v_{abc,right}^{sec,i+1}(t) \tag{14}$$

$$0 = i_{abc,left}^{sec,i}(t) + i_{abc,right}^{sec,i+1}(t) \tag{15}$$

where $i \neq m$. The above voltage and current relationships represent the physical laws (Kirchhoff's voltage and current law). However, at the fault point only the voltage relationships (equation (14)) persist, while the current relationships remain unclear if the fault type is unknown.

$$0 = v_{abc,left}^{f}(t) - v_{abc,right}^{f}(t) \tag{16}$$

Equations (14)–(16) are included in an EnKF DSE process. The results provide an approximate value of fault location $\hat{\alpha}$, as well as the estimated three-phase voltages v_{abc}^{f} at the fault point with which we can classify the type of the fault.

Generally, the smaller the fault impedance is, the larger the change in faulted phase voltage is, and thus the easier the fault classification is. Here we selected four types of impedance fault scenarios (A-G, AB, AB-G, and ABC) at the mid-point of a 200-km transmission line where the fault impedance is 15 Ω. The fault happens at time 0.01 sec. Fig. 2 shows the estimated fault-point voltages for different fault types using the EnKF-based method.

The fault type is determined by checking the three-phase voltages. In Fig. 2(a), the phase B and C voltages are equal to nominal values, while the phase A voltage is very small; thus it is an A-G fault. In Fig. 2(b), the phase C voltage is equal to nominal values, while the phase A and B voltages are the

TABLE I
PARAMETERS OF TRANSMISSION LINE AND EQUIVALENT SYSTEM

l	200-km	V	500-kV
$z_{1,Line}$	(0.01273 + j0.3520) Ω/km	$c_{1,Line}$	12.74 nF/km
$z_{0,Line}$	(0.3864 + j1.5557) Ω/km	$c_{0,Line}$	7.751 nF/km
$z_{1,SL}$	(1.1547 + j11.5473) Ω/km	$z_{1,SR}$	$2z_{1,SL}$
$z_{0,SL}$	(2.8868 + j20.2078) Ω/km	$z_{0,SR}$	$2z_{0,SL}$
Ang_{SL}	0°	Ang_{SR}	−30°

same and close to half of nominal values; thus it is an AB fault. Fig. 2(c) is similar to (b), but the phase A and B voltages are very small (close to zero); thus it is an AB-G fault. In Fig. 2(d), all three phase voltages are small (almost zero), thus it is an ABC fault. In this way, the first step determines the fault type and an initial estimation of the fault location $\hat{\alpha}$.

In the second step, a reinforced EnKF is performed by re-running the DSE process with additional information. With the knowledge of fault type from the first step, additional current relationships at the fault point are derived similar to equations (14)–(16). For example, if the first step determines the fault is an A-G fault, additional current relationships are

$$0 = i^f_{b,left}(t) + i^f_{b,right}(t) \tag{17}$$

$$0 = i^f_{c,left}(t) + i^f_{c,right}(t) \tag{18}$$

The above information can be included as extra constraints (or measurements) when re-running the reinforced EnKF-based DSE, which helps increase the measurement redundancy of the state estimation process.

A good guess of the initial values will increase the accuracy of DSE results, as well as minimize the length of required data window. The estimated fault location $\hat{\alpha}$ in the first step is used as the initial guess of the reinforced EnKF state estimation process. Therefore, when we re-run the reinforced EnKF-based DSE process, it achieves a more accurate estimation of the fault location because of better initial states and increased measurement redundancy [6].

III. TEST RESULTS

To validate the effectiveness of the EnKF-based fault location approach, two groups of fault scenarios were tested on a 500-kV, 200-km transmission line. The parameters of the line and terminal equivalent systems are listed in Table I. The first scenario is a single-phase (phase A) to ground fault, where the fault impedance is 15 Ω. The second one is a bolted phase-to-phase (B-C) fault, where the fault impedance is 0.01 Ω. The proposed EnKF-based approach was compared with the conventional single-ended and dual-ended impedance methods [1] for every 20-km of distance. The process noise for the EnKF-based method is 0.1% [7]. The measurement noise is 1% according to IEEE Standard [8]. The sampling rate is 80 samples per cycle. The results are shown in Tables II and III.

In the first scenarios, where 15 Ω impedance faults occur on phase A-G, the average fault location error for the proposed EnKF-based approach is 0.159 km, and the average errors for conventional single-ended and dual-ended impedance method are 2.614 km and 0.765 km, respectively. The EnKF-based approach gives a maximum error of 0.242 km, while the values for the other two methods are 7.879 km and 1.366 km.

TABLE II
FAULT LOCATION FOR PHASE A-N FAULT, 15 Ω IMPEDANCE

Actual Distance (km)	**EnKF**	**Single-ended**	**Dual-ended**
20	20.144	21.524	21.366
40	40.150	41.023	41.042
60	60.112	60.417	60.722
80	79.846	79.687	80.373
100	99.950	98.814	100.008
120	120.184	117.756	119.642
140	140.178	136.423	139.294
160	160.214	154.635	158.980
180	180.242	172.121	178.709
Average Error (km)	0.159	2.614	0.765

TABLE III
FAULT LOCATION FOR BOLTED PHASE B-C FAULT, 0.01 Ω IMPEDANCE

Actual Distance (km)	**EnKF**	**Single-ended**	**Dual-ended**
20	20.073	19.965	19.058
40	40.021	40.010	39.072
60	59.902	60.000	59.302
80	79.889	80.090	79.755
100	99.891	100.557	100.006
120	119.874	120.728	120.331
140	139.940	141.708	140.858
160	159.801	162.591	161.183
180	179.820	182.994	181.218
Average Error (km)	0.109	0.968	0.712

In the second scenarios where bolted faults occur on phase B-C, the average fault location error for the proposed EnKF-based approach is 0.109 km, and the average errors for the conventional single-ended and dual-ended impedance method are 0.968 km and 0.712 km, respectively. The EnKF-based approach gives a maximum error of 0.199 km, while the values for the other two methods are 2.994 km and 1.218 km.

Remark 1: from the results we can see the EnKF approach persists consistent high accuracy for fault location independent of the fault type or fault impedance.

Remark 2: both conventional impedance methods use only fundamental-frequency phasor values and filter out the high-frequency or DC components. The results in Tables II and III are the average values of the estimated distances calculated from the third cycle measurements (to get rid of large transients) after the fault incipience. However, it will introduce large errors if the fault is quickly tripped and only short-period measurements (with large transients) are available. In contrast, the EnKF-based approach uses instantaneously sampled values instead of phasors, and experimental results show this method will reach a converged solution in half cycle time. Therefore, the EnKF-based approach is much superior when only short-period measurements are available.

IV. Conclusion

This letter proposes a simple yet effective EnKF-based fault location approach. The approach can be easily implemented without explicitly deriving the Jacobian matrix. It does not require foreknowledge of either the fault type or an approximate guess of the fault location. This approach converges fast (in half cycle), so it is superior to conventional impedance methods when only short-period fault measurements are available. Test results validate that the EnKF-based approach can accurately locate faults on transmission lines.

References

[1] *IEEE Guide for Determining Fault Location on ac Transmission and Distribution Lines*, IEEE Std C37.114-2014 (Revision of IEEE Std C37.114-2004), Jan. 2015.

[2] Y. Chen, D. Liu, and B. Xu, "Wide-area traveling wave fault location system based on IEC61850," *IEEE Trans. Smart Grid*, vol. 4, no. 2, pp. 1207–1215, Jun. 2013.

[3] Y. Liu, A. S. Meliopoulos, Z. Tan, L. Sun, and R. Fan, "Dynamic state estimation-based fault locating on transmission lines," *IET Generation, Transmiss. Distrib.*, vol. 11, no. 17, pp. 4184–4192, 2017.

[4] G. Burgers, P. Jan van Leeuwen, and G. Evensen, "Analysis scheme in the ensemble Kalman filter," *Monthly Weather Rev.*, vol. 126, no. 6, pp. 1719–1724, 1998.

[5] R. Huang *et al.*, "Calibrating parameters of power system stability models using advanced ensemble Kalman filter," *IEEE Trans. Power Syst.*, vol. 33, no. 3, pp. 2895–2905, May 2018.

[6] F. Zhang *et al.*, "Impacts of initial estimate and observation availability on convective-scale data assimilation with an ensemble kalman filter," *Monthly Weather Rev.*, vol. 132, no. 5, pp. 1238–1253, 2004.

[7] N. Zhou, D. Meng, Z. Huang, and G. Welch, "Dynamic state estimation of a synchronous machine using PMU data: A comparative study," *IEEE Trans. Smart Grid*, vol. 6, no. 1, pp. 450–460, Jan. 2015.

[8] K. Martin *et al.*, "Exploring the IEEE standard C37. 118–2005 synchrophasors for power systems," *IEEE Trans. Power Del.*, vol. 23, no. 4, pp. 1805–1811, Oct. 2008.